Vol. **1**, **3**. 171-203 (2002)

Revue de Mécanique Appliquée et Théorique

Homogenized models for the modelling of instability in long fibre media

C. Gardin
Laboratoire de Physique et Mécanique des Matériaux, UMR CNRS 7554, Institut Supérieur de Génie Mécanique et Productique, Université de Metz, Île du Saulcy, F-57045 METZ CEDEX 01, France
gardin@lpmm.univ-metz.fr :

M. Potier-Ferry
Laboratoire de Physique et Mécanique des Matériaux, UMR CNRS 7554, Institut Supérieur de Génie Mécanique et Productique, Université de Metz, Île du Saulcy, F-57045 METZ CEDEX 01, France
potier-ferry@lpmm.univ-metz.fr

J.C. Grandidier
Laboratoire de Mécanique et Physique et Mécanique des Matériaux, UMR CNRS 661 École Nationale Supérieure de Mécanique et Aéronautique Téléport 2 ; 1, Avenue Clément Ader, B.P. 4017, F-86961 FUTUROSCOPE-CHASSEINEUIL CEDEX, France
grandidier@lmpm.ensma.fr

Résumé
Dans ce papier, on présente une justification mathématique des modèles de microflambage élastique avec effet de structure. La méthode des échelles multiples est utilisée avec deux petits paramètres (rapport classique d'échelle et rapport de rigidité matrice/fibre), ce qui en constitue l'originalité. Sur la base de ces résultats, un modèle macroscopique (homogène) de microflambage est construit et justifié. Les déformations critiques et les longueurs d'onde de l'instabilité prévues par ce modèle sont proches de celles calculées par Drapier et al. [13] en discrétisant la microstructure du composite à l'aide de la méthode des éléments finis.

Abstract
In this paper, a mathematical justification of elastic microbuckling model with structural effect is proposed. The multiple scale method is used with two small parameters (classical scale ratio and ratio between matrix/fibre stiffness), that is the main originality of this work. From those results, a macroscopic (homogeneous) model of microbuckling is derived. The critical strains and wavelengths obtained with this model are very close to the values calculated by Drapier el al. [13] by discretization of the micro-structure (fibre and matrix) in finite elements.

1. INTRODUCTION

The number of papers concerning the modelling of instability in long fibre heterogeneous media is considerable since the year 1964 in which Rosen [1] has presented the first microbuckling model. The authors study the stability on a microscopic scale, and yet several works (Schaffers [2], Budiansky [3], Grandidier and Potier-Ferry [4], Gardin and Potier-Ferry [5], Guynn [6], Swanson [7], Budiansky and Fleck [8], Wisnom [9], Fleck et al. [10], Fleck and Shu [11], Kyriakides et al. [12], Drapier et al. [13], Drapier et al. [14] and Drapier et al. [15] have shown for example that the phenomenon wavelength is

Received 21 March 2002
Revised 3 June 2002

related to characteristic lengths defined on a macroscopic scale (ply thickness) and on a microscopic scale (fibre gyration radius). Drapier et al. [13] determine the microbuckling mode by discretizing the whole microstructure and show the existence of a boundary layer near a free face. This edge effect takes an important part in the growth of plastic instabilities as underlined by Drapier et al. [14] and Drapier et al. [15]. In order to avoid a complete discretization of the microstructure, these authors propose to represent the material macroscopic behaviour by an equivalent homogeneous medium. This approach has two immediate interests : first it leads in some cases to analytical expressions of the microbuckling stress, and second it gives a simplified buckling modelling. The equilibrium is described by the principle of virtual powers which is presented in the following particular form :

$$-\int_{\Omega} \{f\, E^F r_{gF}^2\, v''\, \delta v'' + S.\delta\gamma\}\, d\Omega + \langle F, \delta u\rangle = 0 \;\forall\; \delta u \qquad (1)$$

The first term of the expression (1) is the virtual power developed by the fibre bending that is distributed in the domain Ω. The fibre curvature is denoted by v'', the fibre Young's modulus is denoted by E^F, the fibre volume fraction by f, and the fibre gyration radius by r_{gF}. The two last terms are more classical, and represent respectively the virtual power of the internal stresses S and the virtual power of the external stresses F acting on the structure.

This approach is undeniably efficient, but the models are often built without mathematical justifications. That is the reason why we want to explain in this paper the origin of the flexion term proposed in equation (1) by a two-dimensional asymptotic analysis. We also aim to build an homogeneous model that could account for the boundary layers observed by Drapier et al. [15] on the microbuckling modes. Our study is based on the multiple scale method, where the small parameter η is nothing else than the parameter classically used in the periodic homogenisation techniques of long fibre composites. The only distinctive feature lies in the choice of the ratio between the matrix and fibre stiffness, which is supposed of the order of η^2 in order to obtain a good estimate of the phenomenon wavelength. By using the results of the asymptotic study, the foundations of the model proposed by Drapier et al. [14] and [15] are presented. In order to complete the validation of our macroscopic model, we test its ability to account for the elastic modes by comparison with the modes obtained by Drapier et al. [13] on the complete microstructure of the composite. The assumptions concerning the displacement field and the microscopic strain field that form the basis for the macroscopic model are then discussed. The shapes of the microbuckling modes and the critical values computed for different structures are compared with those obtained by Drapier et al. [13], which allows us to test the model.

2. TWO-DIMENSIONAL ASYMPTOTIC STUDY

In this section, we consider a bidimensional stack of stiff and soft layers in the plane (x_1, x_2), see Figure 1. The transverse direction through the thickness of the specimen is denoted by x_2, and x_1 is the principal direction of loading. The two-dimensional asymptotic model is derived from plane orthotropic elasticity with geometrical nonlinearities.

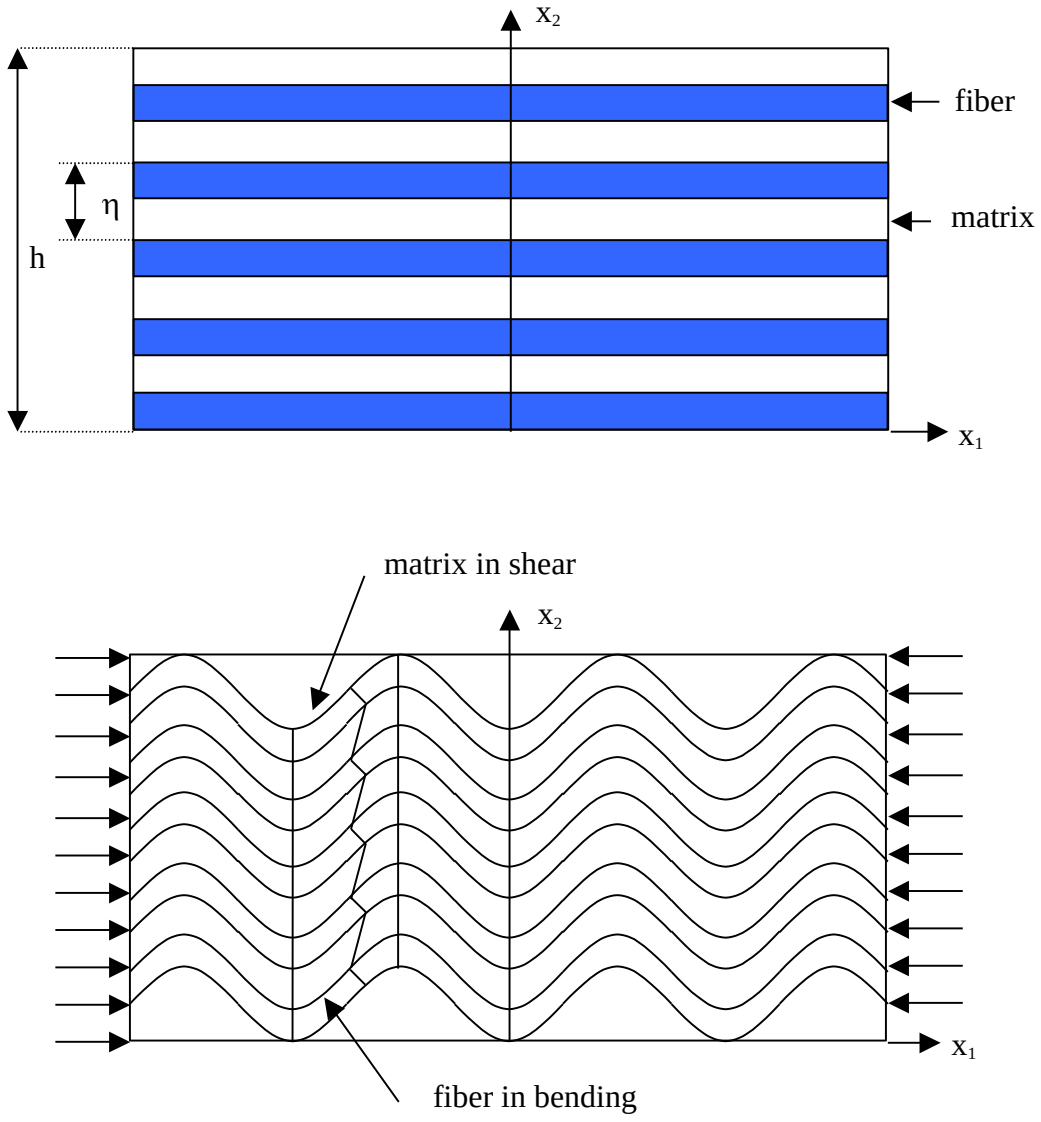

Figure 1 : Geometry without and with deformation

The microbuckling is analysed in the framework of small prebuckling strains and linear buckling [16]. According to these assumptions, the microbuckling mode is solution of the equilibrium equations, that are linearized around a uniaxial stress state Σ applied in the direction x_1 :

$$\frac{\partial \sigma_{\alpha\beta}}{\partial x_\beta} - \Sigma \frac{\partial^2 u_\alpha}{\partial x_1^2} = 0 \text{ with } \alpha = 1, 2 \qquad (2)$$

where σ is the incremental stress tensor and u the displacement field.
The fibre and the matrix are supposed to have a linear and orthotropic behaviour :

$$\begin{pmatrix} \varepsilon_{11} \\ \varepsilon_{22} \\ \varepsilon_{12} \end{pmatrix} = \begin{pmatrix} \frac{1}{E_1} & -\frac{\nu}{E_1} & 0 \\ -\frac{\nu}{E_1} & \frac{1}{E_2} & 0 \\ 0 & 0 & \frac{1}{2G} \end{pmatrix} \begin{pmatrix} \sigma_{11} \\ \sigma_{22} \\ \sigma_{12} \end{pmatrix} \tag{3}$$

where E_1 and E_2 are the Young's moduli in the directions x_1 and x_2, G is the shear modulus in the plane (x_1, x_2) and ν the Poisson's coefficient in the plane (x_1, x_2). These moduli are supposed to take constant values in the fibre and in the matrix. As usual ε is the linearized strain tensor.

It is necessary to add the transmission conditions, which express the continuity of the displacement and the normal stress vector at the fibre-matrix interfaces :

$$\begin{cases} \sigma_{\alpha 2}^{F} = \sigma_{\alpha 2}^{M} \\ u_{\alpha}^{F} = u_{\alpha}^{M} \end{cases} \tag{4}$$

2.1 Setting of the asymptotic expansions

Two small parameters are a priori involved in this problem. The first one is the stiffness ratio (the stiffness of the matrix divided by the stiffness of the fibre), and the second one is the ratio between the microscopic and macroscopic scales. The microscopic scale is the distance between two fibres. In a laminate plate, the macroscopic scale is related to the ply thickness or to the plate thickness (cf. Grandidier et al. [17] and section 5 for analysis of the boundary conditions). It is certainly not evident that the macroscopic scales are the same in the direction of fibres and in the transverse direction, but it is this choice which leads to the richest final model. It is worthwhile to notice that the characteristic length in the direction of fibres is not the length of the plate, but a microbuckling wavelength which is then a consequence of the instability and not a structural data. Experimentally, the microbuckling wavelength is very small compared to the length of the plate (cf. Grandidier et al., [18]). The small parameter which is characteristic from the ratio between the two scales is the distance between two neighbouring fibres and is denoted by η. The microscopic variable is defined by $y_2 = x_2 / \eta$. Therefore, it describes the [-f/2, 1-f/2] interval on one material period, f being the volume fraction of fibres (see Figure 2).

According to previous studies (cf. Grandidier and Potier-Ferry [4]) and taking the preceding hypotheses into account, the stiffness ratio must be chosen of order η^2. Then, let us define :

$$E_1^M = e_1^M \eta^2 \quad ; \qquad E_2^M = e_2^M \eta^2 \quad ; \qquad G^M = g^M \eta^2 \tag{5}$$

where e_1^M, e_2^M and g^M are supposed of order one (as well as the stiffness moduli of the fibre).

According to the constitutive law (3) and the continuity of the displacement (4), it follows that the

axial strain of fibres and axial displacement are of order one. Moreover, the two terms of the shear strain in the matrix must be of the same order ($1/\eta$), which is in accordance with the Rosen's model, in the sense that the shear of the matrix compensate locally for the bending of the fibres in order to avoid a global bending (see Figure 1). It follows that the u_2 displacement is of the order $1/\eta$ and that the shear stress in the matrix is of the order η.

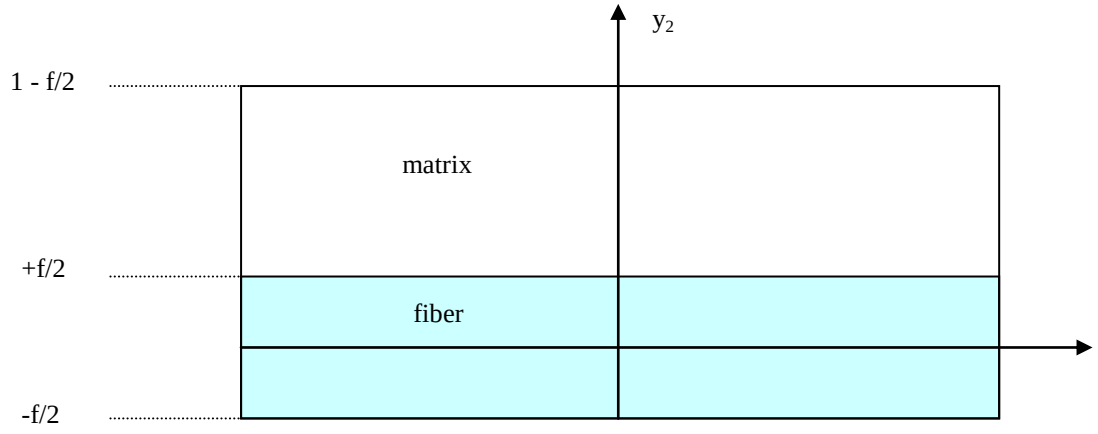

Figure 2: Material period.

Furthermore, it is logical to choose the fibre strain before buckling Σ^F of the order η^2 since, according to Rosen's model, it is expected to find the critical strain of compression of the same order than the shear modulus of the matrix. Thus, we set :

$$\Sigma^F = \sigma^F \eta^2 \tag{6}$$

where σ^F is of order one.

Using the multiple scale method and taking into account the previously established hypotheses, displacement, stresses and strains are sought in the form of series :

$$\begin{cases} u_1 = u_1^0 + \eta\, u_1^1 + \ldots, u_2 = \eta^{-1} u_2^{(-1)} + u_2^0 + \ldots \\ \sigma = \sigma^0 + \eta\, \sigma^1 + \eta^2 \sigma^2 + \ldots \\ \varepsilon = \eta^{-1} \varepsilon^{(-1)} + \varepsilon^0 + \eta\, \varepsilon^1 + \ldots \end{cases} \tag{7}$$

with :

$$\begin{cases} \sigma^0 = 0 \text{ in the matrix} \\ \varepsilon^{(-1)} = 0 \text{ in the fibre} \end{cases} \tag{8}$$

The multiple scale method is based on the following features (cf. Sanchez-Palencia [19]....) :

- All the fields in (7) are periodic of period one with respect to the microscopic variable y_2.

- The derivatives with respect to x_2 are developed using the rule of derivation :

$$\frac{\partial}{\partial x_2} \equiv \frac{\partial}{\partial x_2} + \frac{1}{\eta}\frac{\partial}{\partial y_2} \tag{9}$$

2.2 Love-Kirchhoff kinematic relations

The hypotheses (7) on the orders of magnitude of the displacement field and the strain tensor are not automatically compatible. Indeed, substitution of the expansions (7) into the definition of the linearized strains tensor and use of (9) give :

$$\begin{cases} \varepsilon_{11} = \dfrac{\partial u_1}{\partial x_1} = \dfrac{\partial u_1^0}{\partial x_1} + \eta \dfrac{\partial u_1^1}{\partial x_1} + .. \\ \varepsilon_{22} = \eta^{-1}\dfrac{\partial u_2}{\partial y_2} + \dfrac{\partial u_2}{\partial x_2} = \eta^{-2}\dfrac{\partial u_2^{(-1)}}{\partial y_2} + \eta^{-1}\left(\dfrac{\partial u_2^{(-1)}}{\partial x_2} + \dfrac{\partial u_2^0}{\partial y_2}\right) + \left(\dfrac{\partial u_2^0}{\partial x_2} + \dfrac{\partial u_2^1}{\partial y_2}\right) + ... \\ 2\varepsilon_{12} = \eta^{-1}\dfrac{\partial u_1}{\partial y_2} + \dfrac{\partial u_1}{\partial x_2} + \dfrac{\partial u_2}{\partial x_1} = \eta^{-1}\left(\dfrac{\partial u_2^{(-1)}}{\partial x_1} + \dfrac{\partial u_1^0}{\partial y_2}\right) + \left(\dfrac{\partial u_1^0}{\partial x_2} + \dfrac{\partial u_2^0}{\partial x_1} + \dfrac{\partial u_1^1}{\partial y_2}\right) + ... \end{cases}$$

Comparing with (7) and equating the term in η^{-2} to zero, we obtain that the first term of the transverse displacement u_2 does not depend on the fast variable y_2 in the fibre and in the matrix, as is usually the case in homogenisation (cf. Sanchez-Palencia [19],...) :

$$u_2^{(-1)}(x) \tag{10}$$

Moreover, the strains of order η^{-1} vanish in the fibre from (8), which implies that the displacement in the fibre at order η^0 is a Love-Kirchhoff type, according to the asymptotic models of plates (cf. Destuynder [20]) :

$$\begin{cases} u_1^0(x, y_2) = U_1^0(x) - \dfrac{\partial u_2^{(-1)}(x)}{\partial x_1} y_2 \\ u_2^0(x, y_2) = U_2^0(x) - \dfrac{\partial u_2^{(-1)}(x)}{\partial x_2} y_2 \end{cases} \text{ in the fiber} \tag{11}$$

where $U_1^0(x)$ and $U_2^0(x)$ are the displacements of the middle of the fibre at order η^0.

2.3 Macroscopic equilibrium equations

To apply the multiple scale method, the expansions (7) are put in the equilibrium equations (2) and the increasing powers of η are identified. The different identifications are collected in the Table 1.

Order	FIBER		MATRIX	
η^{-1}	$\frac{\partial \sigma^0_{\alpha 2}}{\partial y_2} = 0$	(F0)		
η^0	$\frac{\partial \sigma^0_{11}}{\partial x_1} + \frac{\partial \sigma^1_{12}}{\partial y_2} = 0$	(F1)	$\frac{\partial \sigma^1_{12}}{\partial y_2} = 0$	(M1)
	$\frac{\partial \sigma^0_{21}}{\partial x_1} + \frac{\partial \sigma^1_{22}}{\partial y_2} = 0$	(F2)	$\frac{\partial \sigma^1_{12}}{\partial y_2} = 0$	(M2)
η^1	$\frac{\partial \sigma^1_{12}}{\partial x_1} + \frac{\partial \sigma^1_{22}}{\partial x_2} + \frac{\partial \sigma^2_{22}}{\partial y_2} - \sigma^F \frac{\partial^2 u^{(-1)}_2}{\partial x_1{}^2} = 0$	(F3)	$\frac{\partial \sigma^1_{12}}{\partial x_1} + \frac{\partial \sigma^1_{22}}{\partial x_2} + \frac{\partial \sigma^2_{22}}{\partial y_2} = 0$	(M3)

Table 1 : Different identifications of the equilibrium equations.

Moreover, combining (4) and (7), the continuity of the displacement and the stress vector at the fibre-matrix interface in the basic cell is fulfilled at each order. We obtain in particular that the stress vector in the fibre is in first approximation equal to zero at the interface, as it is done when modelling beams or plates (cf. Destuynder [20]) :

$$\sigma^{F0}_{\alpha 2} = 0 \quad \text{in } y_2 = f/2 \text{ and } \forall\, x \tag{12}$$

It is very easy to find from equations (F0) of the Table 1 that σ^0_{12} and σ^0_{22} do not depend on y_2 in the fibre. By use of (12), the stress tensor in the fibres at order η^0 is then found to be a tension-compression tensor in the direction of fibres :

$$\sigma^0 = \sigma^0_{11}(x, y_2)\ e_1 \otimes e_1 \text{ in the fiber} \tag{13}$$

Equations (M1), (M2) and (F2) of table 1. imply also in a very simple manner that the shear and transverse stresses are constant at the first order :

$$\begin{cases} \sigma^1_{12}(x) \text{ in the matrix} \\ \sigma^1_{22}(x) \text{ in the matrix and in the fiber} \end{cases} \tag{14}$$

Equations (10), (11) and (13) show that the displacement and the stresses in the fibre identify, locally and at first order, with the equations of an elastic beam. It is then natural to introduce the normal force $<\sigma_{11}>$, the bending moment $< y_2\, \sigma_{11}>$ and the shear force $<\sigma_{12}>$ respectively by :

$$<\sigma_{11}> = \int_{-f/2}^{1-f/2} \sigma_{11}^{0}(x, y_2)\, dy_2 = \int_{-f/2}^{f/2} \sigma_{11}^{0}(x, y_2)\, dy_2 = f\, <\sigma_{11}>^{F} \tag{15}$$

$$< y_2\, \sigma_{11}> = \int_{-f/2}^{1-f/2} \sigma_{11}^{0}\, y_2\, dy_2 = \int_{-f/2}^{f/2} \sigma_{11}^{0}\, y_2\, dy_2 \tag{16}$$

$$\begin{aligned} <\sigma_{12}> &= \int_{-f/2}^{1-f/2} \sigma_{12}^{1}(x, y_2)\, dy_2 = \int_{-f/2}^{f/2} \sigma_{12}^{1}(x, y_2)\, dy_2 + \int_{f/2}^{1-f/2} \sigma_{12}^{1}(x)\, dy_2 \\ &= f\, <\sigma_{12}>^{F} + (1 - f)\, <\sigma_{12}>^{M} \end{aligned} \tag{17}$$

Integration of (F1) and (M1) over the fibre and the matrix respectively gives by addition :

$$\frac{\partial <\sigma_{11}>}{\partial x_1} + [\sigma_{12}^{1}]_{-f/2}^{+f/2} + [\sigma_{12}^{1}]_{+f/2}^{1-f/2} = 0 \tag{18}$$

where $[\,.\,]_{-f/2}^{+f/2}$ denotes the jump over the fibre and $[\,.\,]_{+f/2}^{1-f/2}$ the jump over the matrix.

By use of the continuity and the periodicity of the shear stress σ_{12}^{1}, the equation (18) reduces to the macroscopic equation :

$$\frac{\partial <\sigma_{11}>}{\partial x_1} = 0 \tag{19}$$

In order to obtain the macroscopic equation for the bending moment $< y_2\, \sigma_{11}>$, we multiply (F1) and (M1) by y_2 and we integrate respectively over the fibre and the matrix, which gives by addition :

$$\frac{\partial < y_2\, \sigma_{11}>}{\partial x_1} + \int_{-f/2}^{f/2} y_2 \frac{\partial \sigma_{12}^{1}}{\partial y_2}\, dy_2 + \int_{+f/2}^{1-f/2} y_2 \frac{\partial \sigma_{12}^{1}}{\partial y_2}\, dy_2 = 0$$

This equation can be rewritten by integration by parts as:

$$\frac{\partial < y_2\, \sigma_{11} >}{\partial x_1} + [\, y_2\, \sigma_{12}^1 \,]_{-f/2}^{+f/2} + [\, y_2\, \sigma_{12}^1 \,]_{+f/2}^{1-f/2} - <\sigma_{12}> = 0$$

The continuity of σ_{12}^1 in $y_2 = f/2$ and use of (14) give finally :

$$\frac{\partial < y_2\, \sigma_{11} >}{\partial x_1} + \sigma_{12}^1 (x, \pm \frac{f}{2}) - <\sigma_{12}> = 0$$

Integration of (F3) and (M3) over the fibre and the matrix respectively gives by use of (10) and (14) :

$$\frac{\partial <\sigma_{12}>}{\partial x_1} + \frac{\partial \sigma_{22}^1 (x)}{\partial x_2} + [\, \sigma_{22}^2]_{-f/2}^{+f/2} + [\, \sigma_{22}^2 \,]_{+f/2}^{1-f/2} - f\, \sigma^F \frac{\partial^2 u_2^{(-1)}(x)}{\partial {x_1}^2} = 0$$

which reduces by use of the continuity and the periodicity of the transverse stress σ_{22}^2 to :

$$\frac{\partial <\sigma_{12}>}{\partial x_1} + \frac{\partial \sigma_{22}^1 (x)}{\partial x_2} - f\, \sigma^F \frac{\partial^2 u_2^{(-1)}(x)}{\partial {x_1}^2} = 0 \qquad (20)$$

2.4 Macroscopic constitutive laws

From the constitutive law (3) and the expression (11) for u_1^0, we obtain that, in the fibre and at the order η^0, the axial stress is linear in y_2 :

$$\sigma_{11}^0 = E_1^F\, \varepsilon_{11}^0 = E_1^F \frac{\partial u_1^0}{\partial x_1} = E_1^F [\, \frac{\partial U_1^0(x)}{\partial x_1} - \frac{\partial^2 u_2^{(-1)}(x)}{\partial {x_1}^2}\, y_2 \,]$$

Substituting this relation into (15) and (16) gives beam-type constitutive laws :

$$<\sigma_{11}> = E_1^F \int_{-f/2}^{f/2} [\, \frac{\partial U_1^0(x)}{\partial x_1} - \frac{\partial^2 u_2^{(-1)}(x)}{\partial {x_1}^2}\, y_2 \,]\, dy_2 = E_1^F\, f \frac{\partial U_1^0(x)}{\partial x_1} \qquad (21)$$

$$< y_2\, \sigma_{11}> = E_1^F \int_{-f/2}^{f/2} [\, \frac{\partial U_1^0}{\partial x_1}\, y_2 - \frac{\partial^2 u_2^{(-1)}}{\partial {x_1}^2}\, {y_2}^2 \,]\, dy_2 = - \frac{E_1^F f^3}{12} \frac{\partial^2 u_2^{(-1)}(x)}{\partial {x_1}^2} \qquad (22)$$

Using the constitutive law of the matrix at order η^{-1}, we obtain in the matrix :

$$\begin{cases} \varepsilon_{11}^{(-1)} = 0 = \dfrac{1}{e_1^M}\sigma_{11}^1 - \dfrac{\nu^M}{e_1^M}\sigma_{22}^1 \\ \varepsilon_{22}^{(-1)} = \dfrac{\partial u_2^{(-1)}(x)}{\partial x_2} + \dfrac{\partial u_2^0}{\partial y_2} = \dfrac{1}{e_2^M}\sigma_{22}^1 - \dfrac{\nu^M}{e_1^M}\sigma_{11}^1 \\ 2\,\varepsilon_{12}^{(-1)} = \dfrac{\partial u_2^{(-1)}(x)}{\partial x_1} + \dfrac{\partial u_1^0}{\partial y_2} = \dfrac{1}{g^M}\sigma_{12}^1 \end{cases} \tag{23}$$

As a first consequence of (14) and (23), we obtain that all the components of the stress tensor σ^1 in the matrix do not depend on y_2. It is then easy to integrate (23) and find the displacement field in the matrix at order η^0, with the help of the continuity and periodicity conditions (see Figure 3), and the stress tensor in the matrix at order η^1 :

$$\begin{cases} u_1^0(x, y_2) = U_1^0(x) + \dfrac{f}{1-f}\dfrac{\partial u_2^{(-1)}}{\partial x_1}\left(y_2 - \dfrac{1}{2}\right) \\ u_2^0(x, y_2) = U_2^0(x) + \dfrac{f}{1-f}\dfrac{\partial u_2^{(-1)}}{\partial x_2}\left(y_2 - \dfrac{1}{2}\right) \end{cases} \quad \text{in the matrix} \tag{24}$$

$$\sigma^1 = \frac{1}{1-f}\begin{pmatrix} \dfrac{\nu^M e^M}{1-\nu^{M2}}\dfrac{\partial u_2^{(-1)}}{\partial x_2} & g^M\dfrac{\partial u_2^{(-1)}}{\partial x_1} \\ g^M\dfrac{\partial u_2^{(-1)}}{\partial x_1} & \dfrac{e^M}{1-\nu^{M2}}\dfrac{\partial u_2^{(-1)}}{\partial x_2} \end{pmatrix} \quad \text{in the matrix} \tag{25}$$

where :

$$\frac{e^M}{1-\nu^{M2}} = \frac{e_1^M e_2^M}{e_1^M - (\nu^M)^2 e_2^M}$$

From (11) and (24) we can now calculate the macroscopic strain tensor :

$$\begin{cases} \langle \varepsilon_{11} \rangle = \displaystyle\int_{-f/2}^{1-f/2} \frac{\partial u_1^0}{\partial x_1}\, dy_2 = f \langle \varepsilon_{11} \rangle^F + (1-f) \langle \varepsilon_{11} \rangle^M = \frac{\partial U_1^0}{\partial x_1} \\ \langle \varepsilon_{22} \rangle = \displaystyle\int_{+f/2}^{1-f/2} \left(\frac{\partial u_2^{(-1)}}{\partial x_2} + \frac{\partial u_2^0}{\partial y_2} \right) dy_2 = (1-f) \langle \varepsilon_{22} \rangle^M = \frac{\partial u_2^{(-1)}}{\partial x_2} \\ \langle 2\,\varepsilon_{12} \rangle = \displaystyle\int_{+f/2}^{1-f/2} \left(\frac{\partial u_2^{(-1)}}{\partial x_1} + \frac{\partial u_1^0}{\partial y_2} \right) dy_2 = (1-f) \langle 2\,\varepsilon_{12} \rangle^M = \frac{\partial u_2^{(-1)}}{\partial x_1} \end{cases} \tag{26}$$

By use of (17) (21), (22), (25) and (26), we obtain finally the macroscopic constitutive laws :

$$\begin{bmatrix} \langle \sigma_{11} \rangle \\ \langle \sigma_{22} \rangle \\ \langle \sigma_{12} \rangle \end{bmatrix} = \begin{bmatrix} f E_1^F & 0 & 0 \\ 0 & \dfrac{e^M}{(1-f)(1-\nu^{M2})} & 0 \\ 0 & 0 & \dfrac{2 g^M}{1-f} \end{bmatrix} \begin{bmatrix} \langle \varepsilon_{11} \rangle \\ \langle \varepsilon_{22} \rangle \\ \langle \varepsilon_{12} \rangle \end{bmatrix} + \begin{bmatrix} 0 \\ 0 \\ -\dfrac{E_1^F f^3}{6} \dfrac{\partial^2}{\partial x_1^2} \langle \varepsilon_{12} \rangle \end{bmatrix} \tag{27}$$

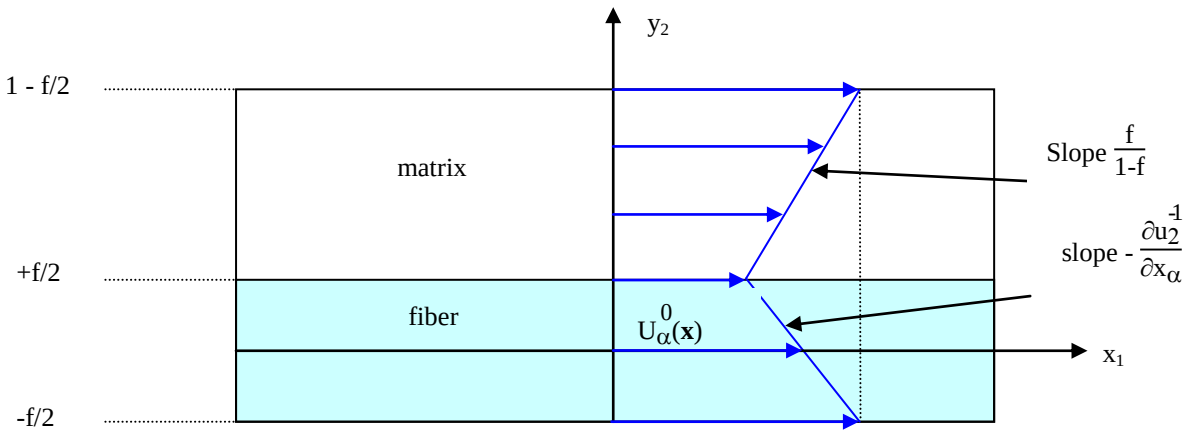

Figure 3: Displacement field $u_\alpha^0(\mathbf{x}, y_2)$.

2.5 Microbuckling equation

Substitution of (25) and (27) into (20) gives the following buckling equation :

$$-\frac{E_1^F f^3}{12}\frac{\partial^4 u_2^{(-1)}(x)}{\partial x_1^4} + \left(\frac{g^M}{1-f} - f\sigma^F\right)\frac{\partial^2 u_2^{(-1)}(x)}{\partial x_1^2} + \frac{e^M}{(1-f)(1-\nu^{M2})}\frac{\partial^2 u_2^{(-1)}(x)}{\partial x_2^2} = 0 \qquad (28)$$

It will be more convenient to reintroduce the physical data in this equation. First, let us suppose now that the fibre and the matrix are isotropic :

$$\begin{cases} E_1^F = E_2^F = E^F \\ E_1^M = E_2^M = E^M \end{cases}$$

Secondly, the fibre gyration radius is defined by :

$$r_{gF} = \sqrt{\frac{I_F}{S_F}} \qquad (29)$$

where I_F and S_F are respectively the quadratic momentum and the fibre surface. This implies here :

$$r_{gF}^2 = \frac{f^2\eta^2}{12}$$

Thirdly, let v(x) be the first approximation of the transverse displacement :

$$u_2^{(-1)}(x) = \eta\, v(x) \qquad (30)$$

Thus, equation (28) becomes by use of (5), (6), (29) and (30) :

$$E^F r_{gF}^2\frac{\partial^4 v(x)}{\partial x_1^4} + \left(\Sigma^F - \frac{G^M}{f(1-f)}\right)\frac{\partial^2 v(x)}{\partial x_1^2} - \frac{E^M}{f(1-f)(1-\nu^{M2})}\frac{\partial^2 v(x)}{\partial x_2^2} = 0 \qquad (31)$$

The two first terms of (31) are similar to those obtained by Rosen, and the third one was already found by Grandidier and Potier-Ferry [4] and shows that the microbuckling depends on the boundary conditions and on the distribution of loading through the thickness. This asymptotic study gives then a new validation of Rosen's model. For thick plies, the third term of equation (31) becomes negligible, and the homogenized model reduces to Rosen's model.

2.6 Solution of the microbuckling equation in the clamped-clamped case

The solution of (31) is valid when the two faces of the domain are clamped. It is possible to search the displacement field in the form :

$$v(x_1, x_2) = V(x_2) \sin kx_1 \tag{32}$$

which corresponds to a cellular instability (see section 4). We obtain by replacing (32) into (31) the following ordinary differential equation :

$$-\left(\frac{E^M}{G^M(1-\nu^{M2})}\right) V''(x_2) + \left[1 + \frac{E^F r_{gF}^2 k^2 f(1-f)}{G^M} - \frac{\Sigma^F f(1-f)}{G^M}\right] k^2 V(x_2) = 0 \tag{33}$$

As it is evident from (32) the boundary conditions($x_2 = 0$, $x_2 = h$) in the clamped-clamped case are :

$$\begin{cases} V(0) = 0 \\ V(h) = 0 \end{cases} \tag{34}$$

It is very easy to solve (33) with the help of (34), which gives :

$$V(x_2) = A \sin\left(\frac{\pi x_2}{h}\right) \tag{35}$$

where A is a constant. Replacing (35) into (33) leads to the neutral stability curve :

$$\Sigma^F(k) = \frac{E^M \pi^2}{f(1-f)(1-\nu^{M2}) h^2} \frac{1}{k^2} + \frac{G^M}{f(1-f)} + E^F r_{gF}^2 k^2$$

The solution is finally obtained by looking for the minimum of Σ^F, which is reached when :

$$k_c = \sqrt[4]{\frac{E^M}{(1-\nu^{M2}) f(1-f) E^F}} \sqrt{\frac{\pi}{h\, r_{gF}}} \tag{36}$$

$$\Sigma_c^F = \frac{G^M}{f(1-f)} + \sqrt{\frac{E^M E^F}{(1-\nu^{M2})} f(1-f)}\ \frac{\pi}{h}\ (2\, r_{gF}) \tag{37}$$

The microbuckling wavenumber (36) depends on the fibre gyration radius and on the thickness h. We have already introduced this characteristic length in Grandidier et al. [17]. This thickness alone accounts the effect of the boundary conditions imposed in the two faces of the ply. The critical stress (37) is expressed as the sum of two terms. The first is the one given by Rosen's model, and the second term accounts the structural effects and becomes significant only for a high ratio between the gyration radius and the thickness of ply.

The equation (31) only holds inside the ply because no boundary layers are observed in the case of clamped faces and therefore the longitudinal strain can be neglected.

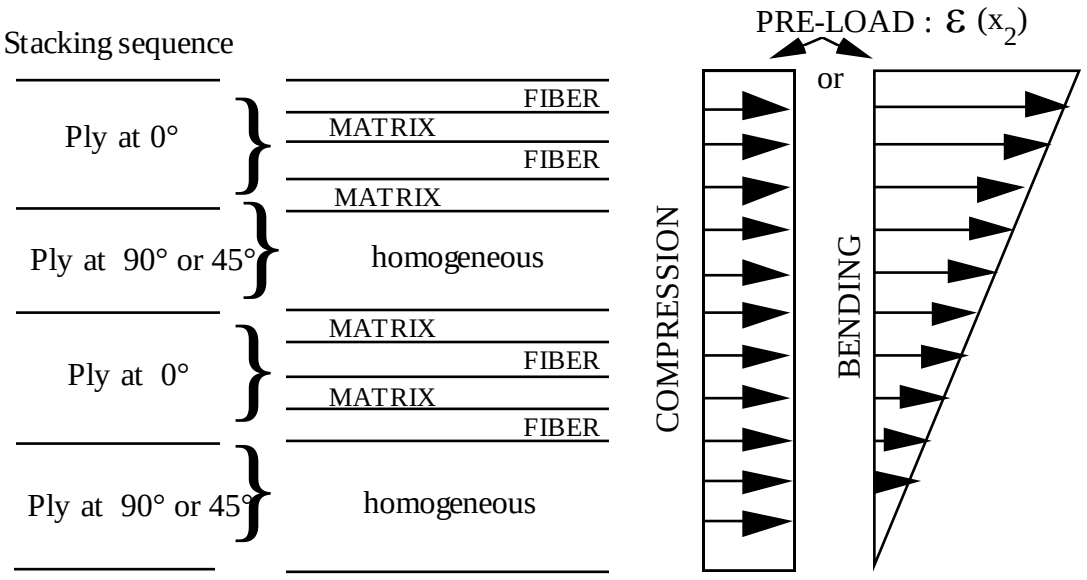

Figure 4 : Two-dimensional modelling of the complete microstructure.

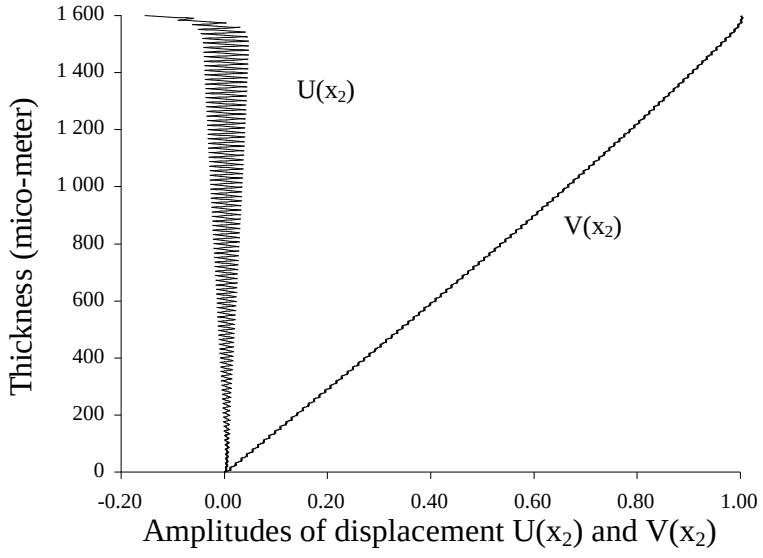

Figure 5 : Shape of modal amplitudes in the case of purely unidirectional composite, complete discretization, compressive load, thickness 1600 μm, boundary conditions : clamped bottom face and free top face.

In the case of free faces, the equation (31) is not exactly the stability equation, because it is not possible to satisfy simultaneously the boundary conditions $\sigma_{11} = 0$ and $\sigma_{12} = 0$. Near the free face (Figure 5), the displacement field in the fibre direction is of the same order than the transverse displacement field. The asymptotic study cannot take this boundary layer into account, because the longitudinal displacement is assumed very small (see the developments (7)). Moreover, the periodicity condition in the boundary layer is in contradiction to the boundary condition at the free face.

It is then necessary to add a study of the boundary layers which appear near the free faces. In the next section we propose to extend this model. The longitudinal displacement u is taken into account and the bifurcation criterion $\delta P_2 = 0$ gives two macroscopic partial differential equations (46) and (47) instead of (31), and so we can model the boundary effects and predict the boundary layers with a macroscopic model.

3. A MACROSCOPIC MODEL FOR MICROBUCKLING

In this section, we propose a two-dimensional model built by extending the results of the preceding asymptotic study. The effect of the boundary conditions on the faces of the ply, that cannot be taken into account by the asymptotic development, is obtained here by supposing the displacement fields in the two directions x_1 and x_2 of the same order of magnitude.

3.1 Potential energy

We have shown previously that the fibre is submitted to a bending-compression state and that its displacement field is of Bernoulli's type (Carbon fibres have a small shear modulus). We suppose that this holds inside the ply as well as in the boundary layer. Splitting up the strain energy into the sum of the bending energy and the membrane energy and supposing a linear prebuckling, the quadratic part of the potential energy is equal to :

$$P_2 = \frac{1}{2} \int_{2\text{-}D} \langle \varepsilon \rangle L^{equ} \langle \varepsilon \rangle \, ds - \int_{2\text{-}D} \langle \sigma^{pb} \rangle \frac{1}{2} {}^t\nabla u \, . \, \nabla u \, ds + W^{bending} \tag{38}$$

where L^{equ} is the stiffness tensor of the classical equivalent homogeneous material and $\langle \sigma^{pb} \rangle$ is the mean prebuckling stress tensor, which generalize the uniaxial stress Σ defined in equation (2). The term $\langle \varepsilon \rangle$ represents the mean microscopic strain tensor in the matrix, and the mean *membrane* strain tensor in the fibre. The bending in fibres gives rise to a strain energy denoted by $W^{bending}$. Considering the fibre Bernoulli's kinematics and the ratios fibre strains over matrix strains, the transverse strain ε_{22} and the shear strain ε_{12} can both be neglected in the fibre :

$$\varepsilon^F_{\alpha 2} = 0 \qquad (\alpha = 1,2)$$

The transverse strain ε_{22} and the shear strain ε_{12} are therefore localised in the matrix and the results of the asymptotic study show that they can be assumed constant. Thus, the mixture rule writes in first approximation :

$$<\varepsilon_{\alpha 2}> = (1 - f)\, \varepsilon^{M}_{\alpha 2} \tag{39}$$

with $<\varepsilon_{22}> = \dfrac{\partial v}{\partial x_2}$ and $<\varepsilon_{12}> = \dfrac{\partial u}{\partial x_2} + \dfrac{\partial v}{\partial x_1}$.

The strains are also supposed constant in x_2 in the matrix and in the fibre (only for the membrane part) as well, which implies :

$$\varepsilon^{F}_{11} = \varepsilon^{M}_{11} = <\varepsilon_{11}> = \frac{\partial u}{\partial x_1} \tag{40}$$

3.2 Equivalent homogeneous constitutive law

To build up the stiffness tensor of the equivalent homogeneous material L^{equ}, the mean stresses must be first calculated by use of the mixture rule :

$$\begin{cases} <\sigma_{11}> = f\ <\sigma^{F}_{11}> + (1 - f)\, \sigma^{M}_{11} \\ <\sigma_{22}> = \sigma^{F}_{22} = \sigma^{M}_{22} \\ <\sigma_{12}> = \sigma^{F}_{12} = \sigma^{M}_{12} \end{cases} \tag{41}$$

Secondly, the microscopic stresses are related to the microscopic strains by use of the constitutive laws in the matrix and in the fibre. For an isotropic matrix, we obtain :

$$\begin{cases} \sigma^{F}_{11} = E^{F}\, \varepsilon^{F}_{11} \\ \sigma^{M}_{11} = \dfrac{E^{M}}{1 - \nu^{M2}}\, \varepsilon^{M}_{11} + \dfrac{E^{M} \nu^{M}}{1 - \nu^{M2}}\, \varepsilon^{M}_{22} \\ \sigma^{M}_{22} = \dfrac{E^{M} \nu^{M}}{1 - \nu^{M2}}\, \varepsilon^{M}_{11} + \dfrac{E^{M}}{1 - \nu^{M2}}\, \varepsilon^{M}_{22} \\ \sigma^{M}_{12} = 2\, G^{M}\, \varepsilon^{M}_{12} \end{cases} \tag{42}$$

Combining equations (39), (40), (41) and (42) leads to the following relation between the mean stresses and strains :

$$\begin{bmatrix} <\sigma_{11}> \\ <\sigma_{22}> \\ <\sigma_{12}> \end{bmatrix} = \begin{bmatrix} f E^F + (1-f)\dfrac{E^M}{1-\nu^{M2}} & \dfrac{E^M \nu^M}{1-\nu^{M2}} & 0 \\ \dfrac{E^M \nu^M}{1-\nu^{M2}} & \dfrac{E^M}{(1-f)(1-\nu^{M2})} & 0 \\ 0 & 0 & \dfrac{G^M}{1-f} \end{bmatrix} \begin{bmatrix} <\varepsilon_{11}> \\ <\varepsilon_{22}> \\ <\varepsilon_{12}> \end{bmatrix}$$

The equivalent stiffness matrix is constructed here in the case of an isotropic matrix, but it is easy to generalise in the case of an orthotropic matrix

3.3 Quadratic part of the homogenized potential energy

The bending energy contained in the fibres is distributed in the 2-D domain, and then is equal to :

$$W^{bend} = \frac{1}{2} f \int_\Omega E^F r_{gF}^2 \left(\frac{\partial^2 v}{\partial x_1^2}\right)^2 d\Omega \tag{43}$$

where r_{gF} is the fibre gyration radius given by (29).

The pre-load tensor is calculated by use of the mixture rule, but as the fibre stiffness is much greater than the matrix one, the prebuckling stresses are neglected in the matrix. Thus, the following relation is obtained :

$$<\sigma^{pb}> = f\, \sigma^{pb\ F} = f\, E^F \varepsilon^{pb\ F} \tag{44}$$

where $\sigma^{pb\ F}$ is the pre-load stress tensor in the fibre. Only the component 11 of this tensor is significant under compression, and depends on the position of the fibre in the laminate under bending.

The prebuckling is then characterised by the tensor :

$$<\sigma^{pb}> = \begin{bmatrix} f E^F \varepsilon_{11}^{pb}(x_2) & 0 \\ 0 & 0 \end{bmatrix}$$

Accounting for all these results, the quadratic part of the homogenized potential energy writes finally :

$$P_2 = \frac{1}{2}\int_\Omega <\varepsilon>.L^{equ}.<\varepsilon>\, d\Omega - \frac{1}{2}\int_\Omega \lambda\, f\, E^F \left(\frac{\partial v}{\partial x_1}\right)^2 d\Omega + \frac{1}{2}\int_\Omega f\, E^F r_{gF}^2 \left(\frac{\partial^2 v}{\partial x_1^2}\right)^2 d\Omega \tag{45}$$

By application of the classical stability criterion $\delta P_2 = 0$, one obtains the two following partial differential equations :

$$\left[f E^F + \frac{(1-f) E^M}{1-\nu^{M2}} \right] \frac{\partial^2 u}{\partial x_1^2} + \frac{E^M \nu^M}{1-\nu^{M2}} \frac{\partial^2 v}{\partial x_1 \partial x_2} + \frac{G^M}{1-f} \left(\frac{\partial^2 u}{\partial x_2^2} + \frac{\partial^2 v}{\partial x_1 \partial x_2} \right) = 0 \qquad (46)$$

$$f E^F r_{gF}^2 \frac{\partial^4 v}{\partial x_1^4} + \left(\lambda f E^F \varepsilon_{11}^d - \frac{G^M}{1-f} \right) \frac{\partial^2 v}{\partial x_1^2} - \frac{E^M}{(1-f).(1-\nu^{M2})} \frac{\partial^2 v}{\partial x_2^2} - \left(\frac{G^M}{1-f} + \frac{E^M \nu^M}{1-\nu^{M2}} \right) \frac{\partial^2 u}{\partial x_1 \partial x_2} = 0 \qquad (47)$$

which must be completed by the boundary conditions imposed on the edge of the domain.
So the asymptotic model (31) does not include the longitudinal displacement u. Nevertheless, we had assumed in the asymptotic approach that the stiffness of the matrix is small with respect to the one of the fibre. By reintroducing this assumption in the first equation (46), we obtain that the longitudinal strain $\frac{\partial u}{\partial x_1}$ is nearly constant and it is clear that this strain can be neglected because of the strong rigidity of the fibre. If we drop the axial displacement in second equation (47), we find the stability equation (31) obtained in the asymptotic framework.
The longitudinal displacement u is added to the model in order to satisfy exactly the boundary conditions which are imposed on the ply faces. We hope in this way to take the effect of the boundary layer better into account. But there is no guarantee that this way to proceed will be sufficient, because the thickness of the boundary layer is of the same order than the size of the constituents (Drapier et al. [13]). Whereas the asymptotic study is based on mathematical foundations, the macroscopic model is built with the help of some assumptions on the microscopic strains that it is important to validate.

4. NUMERICAL VALIDATION OF THE MACROSCOPIC MODELS

In this section the microscopic strains are evaluated by means of modal computations performed on the complete microstructure. The validity of the assumptions on which the macroscopic model is based (displacement field and strain tensor) is established. Furthermore the critical modes and strains resulting from the macroscopic model are compared with those obtained by Drapier et al. [13].

4.1 Study of modal microscopic fields

Drapier et al. [13] have considered a bidimensional stack of stiff and soft layers in the plane (x_1, x_2), see Figure 4. As in section 2, the transverse direction through the thickness of the specimen is denoted by x_2, and x_1 is the principal direction of loading (referred as 0°). In 0° plies, each individual fibre is represented by a hard layer with its real diameter, and the thickness of soft layers is chosen to get a prescribed volume fraction of fibres f. As for the 90° or 45° plies, they are represented by an equivalent homogeneous material, whose characteristics are calculated by use of the mixture rule. The model is derived from plane orthotropic elasticity with geometrical nonlinearities as in section 2, and there is no a priori assumption about displacement and strain fields. Each constituent is supposed here to have a linear elastic and isotropic behaviour. The microbuckling is analysed in the framework of small prebuckling strains and linear buckling. According to these assumptions, the microbuckling mode is solution of the linearized equilibrium equations (2), that are rewritten in the form :

$$\frac{\partial \sigma_{\alpha\beta}}{\partial x_\beta} - \lambda \Sigma (x_2) \frac{\partial^2 u_\alpha}{\partial x_1^2} = 0$$

where λ is the load parameter. In this paper, we do not consider bending and we limit ourselves to pure compression in which case $\Sigma (x_2)$ is equal to the Young's modulus $E(x_2)$.

As Drapier et al. [13], we suppose that microbuckling is a cellular instability. Indeed, from the experimental observations of Grandidier et al. [17], the microbuckling wavelengthes in the fibre direction are in the range 100μm - 1000μm, that is to say much smaller than the length of the specimen. The modes are thus searched in the following particular form :

$$\begin{cases} u (x_1, x_2) = U (x_2) \cos kx_1 \\ v (x_1, x_2) = V (x_2) \sin kx_1 \end{cases} \tag{48}$$

where k denotes the wavenumber and $U(x_2)$,$V(x_2)$ the amplitudes of the displacement field. Putting this displacement field into the equilibrium equation and integrating with respect to x_1 on one wavelength, it remains a unidimensional eigenvalue problem that has been solved by the Finite Element Method. For each imposed value of the wavenumber, the first eigenvalue is computed. The neutral stability curve $\lambda(k)$ is obtained making the wavenumber vary. The minimum of this curve corresponds to the critical strain and the critical wavenumber of microbuckling.

Drapier et al. [13] have established that microbuckling depends on structural data, but here we will study only the influence of the specimen thickness by considering two cases : a thick unidirectional layer (h = 1600μm) and a thin unidirectional layer (h = 160μm). The mechanical characteristics are shown in Table 2. The bottom face of the ply is assumed clamped and the top face is free to study the displacement and strain fields in the boundary layer.

Isotropic matrix	$E^M = 4.5$ GPa $G^M = 1.6$ GPa $\nu^M = 0.4$
Anisotropic fibre	$E_1^F = 240$ GPa, $E_2^F = 15$ GPa $G^F = 92$ GPa $\nu^F = 0.3$
Volume fraction	$f = 0.625$
Diameter of fibres	$D_f = 10$ μm
Ply thickness	h = 1600 μm or 160 μm
Boundary conditions	bottom face clamped top face free

Table 2: Mechanical characteristics.

In Figure 5 the amplitudes U and V of the "exact" microbuckling mode are plotted versus x_2 in the case of a thick unidirectional under pure compression. Inside the ply, the distribution of the amplitude through the thickness is nearly periodic in x_1 and nearly linear in x_2. The mean amplitude U is distinctly lower than V (1.48% at the middle of ply), which is in perfect agreement with the results of the asymptotic study. Only the amplitude of the longitudinal displacement U varies noticeably inside the boundary layer (Figure 6) and reaches 10.7% on the face, which is comparable with the amplitude V. This strong variation of the amplitude U is linear in x_2 in the few fibres nearest the face, whereas $V(x_2)$ is constant in first approximation. This allows to consider that the Bernoulli's assumption is still valid inside the boundary layer.

From this displacement field, different ratios between strain components in the matrix and in the fibre are deduced and presented in Table 3 in both cases of thick and thin layers. Here only the maximal strains are retained.

		A	B	C	D	E
		$\frac{\varepsilon_{12}^f}{\varepsilon_{11}^f} =$	$\frac{\varepsilon_{11}^m}{\varepsilon_{12}^m} =$	$\frac{\varepsilon_{11}^m}{\varepsilon_{22}^m} =$	$\frac{\varepsilon_{22}^m}{\varepsilon_{12}^m} =$	$\frac{\varepsilon^f}{\varepsilon_{12}^m} =$
Thick layer	Isotropic fibre	0.47	0.035	0.30	0.13	0.038
	Anisotropic fibre	1.32	0.03	0.25	0.14	0.04
Thin layer	Isotropic fibre	0.19	0.096	0.41	0.24	0.13
	Anisotropic fibre	0.89	0.13	0.64	0.21	0.14

Table 3: Different ratios between strain components in the matrix and in the fibre.

In the matrix, it appears that the largest modal strain (columns BCD) is the shear strain, as expected from Rosen's analysis and asymptotic development. The transverse strain is about 13% - 24% with respect to the shear strain (D), but it can never be neglected. The longitudinal strain is also not too small, at least for a thin layer (1%). It appears clearly that the preponderance of the shear strain is more significant for a thick layer, which means that, in this case, the classical Rosen's assumptions are more valid than for a thin layer. Similar remarks can be made in the case of an anisotropic fibre. The distribution of strains through the specimen thickness is also studied and it appears that the main strain components (ε_{12} and ε_{22}) in the matrix are about constant on each basic cell as we supposed in the macroscopic model.

The largest strain component in the fibre is less than 15 % of the matrix shear strain for a thin layer and is very small for a thick layer (column E). Hence the strains in the fibre must be taken into account if the ply thickness is sufficiently small. In the fibre, the transverse strain can always be neglected and the shear and longitudinal strains have the same order of magnitude. If the shear strain seems locally constant, the longitudinal strain is approximately linear. So the strain field in the fibre could more or less be given by Timoshenko beam approximations. Only this result is in contradiction with the

asymptotic study and can be explained by the small shear stiffness of Carbon fibres compared to their axial stiffness.
So the detailed modal description confirms the influence of thickness effects on instability. Microbuckling is mainly governed by matrix shear strain, as it is classically assumed. Nevertheless, except for the transverse fibre strain, any component of the shear strain must be taken into account, especially for thin specimens.
The assumptions on which the macroscopic model is based are very related to the results of this microscopic study.

4.2 Validation of the elastic mode

The microbuckling mode and the critical strain are calculated by solving the bifurcation criterion $\delta P_2=0$. The quadratic part of the potential energy (45) includes not only first derivatives of the displacement but also a second derivative with respect to x_1. Thus, a 2-D discretization is complex because the interpolation must be of Lagrange's type in the transverse direction x_2, and of Hermite's type in x_1. To avoid this problem and to make the comparison between the homogenized and heterogeneous models easier, the modes are still searched in the form (48). With such a displacement field, it is sufficient to discretize the domain only in its thickness into a series of 1-D finite elements. Finite elements having three nodes and a Lagrange quadratic interpolation in the x_2 direction are used. The degrees of freedom at each node are the amplitudes $U(x_2)$ and $V(x_2)$. The elementary elastic stiffness and geometric non-linearity matrices are explicitly computed by a symbolic calculation code. Indeed, these matrices are not classical because the modes have sine or cosine shapes in the x_1 direction, and in addition, the quadratic part of the potential energy contains a bending term (second derivative in x_1). Unlike the complete discretization, the 0° plies are homogeneous. The number of elements only depends on the ply thickness (it does not depend on the ply microstructure). Practically, a single element contains several fibre-matrix couples. The 90° or 45° plies are represented by a classical homogeneous and isotropic medium where the fibre bending and nonlinearity terms are excluded. More precisely, the quadratic part of the potential energy reduces to the classical 2-D strain energy. By this fact, the instability is supposed to appear only in 0° plies, the transverse layers behaving like elastic supports. As before we seek the neutral stability curve $\lambda(k)$ whose minimum corresponds to the critical load and the critical wavenumber of microbuckling for the macroscopic model.
Now, we analyse in details the modal shapes that are obtained from this heterogeneous model in the case of a thin and of a thick layer.
A series of computations has been performed on UD composites whose characteristics are presented in Table 2. The results of the homogenized model are systematically in very good agreement with the results of the complete discretization, for any thicknesses and boundary conditions. As for the mode, the mean distribution of the displacement through the thickness is well represented by the homogenized model (see Figures 5 and 7). The homogenized model describes correctly the distribution of the displacement in the boundary layer near the top face, although the thickness of the boundary layer is small in comparison with the heterogeneity size. Indeed, about three fibre-matrix couples are affected by the edge effect. In Figure 8, the 1600 μm thick composite is clamped on its top face, and the comparison between the homogenized model and the complete discretization is still excellent. As the ply thickness decreases to 64 μm (clamped bottom face and free top face), the homogenized model still gives coherent information on the mode (Figure 9). At 64 μm, the ply is constituted of four fibres and four matrix layers. At this level, the notion of equivalent homogeneous

medium is very questionable, but the displacement fields and the orders of magnitude are still comparable, which partly justifies the good correlation between the two models.

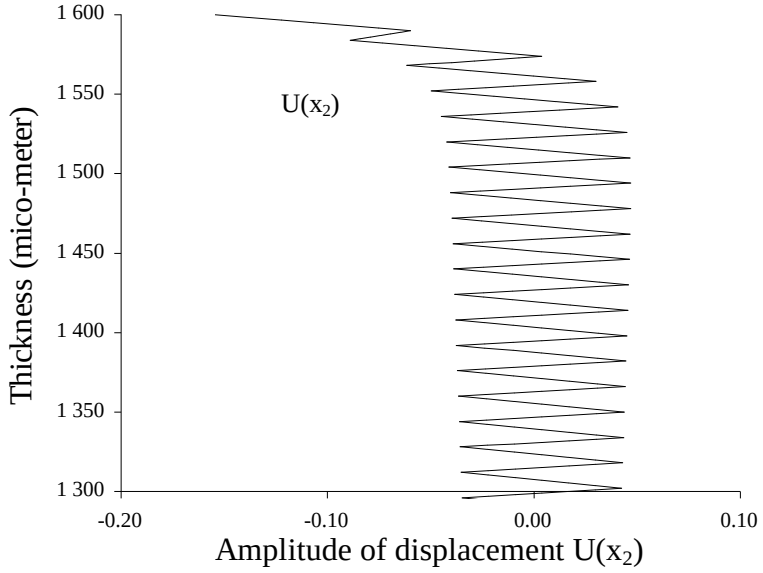

Figure 6 : Zoom of modal amplitude $U(x_2)$ in the case of purely unidirectional composite, complete discretization, compressive load, thickness 1600 μm, boundary conditions : clamped bottom face and free top face.

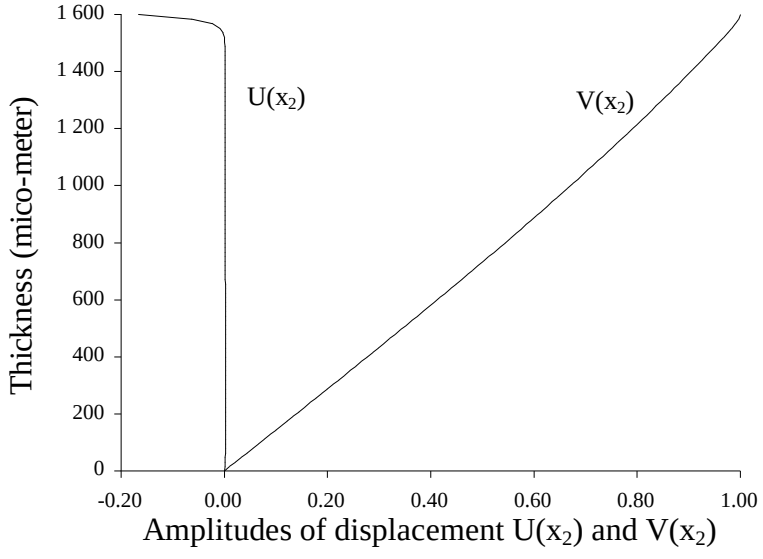

Figure 7 : Shape of modal amplitudes in the case of purely unidirectional composite, macroscopic model, thickness 1600 μm, boundary conditions : clamped bottom face and free top face.

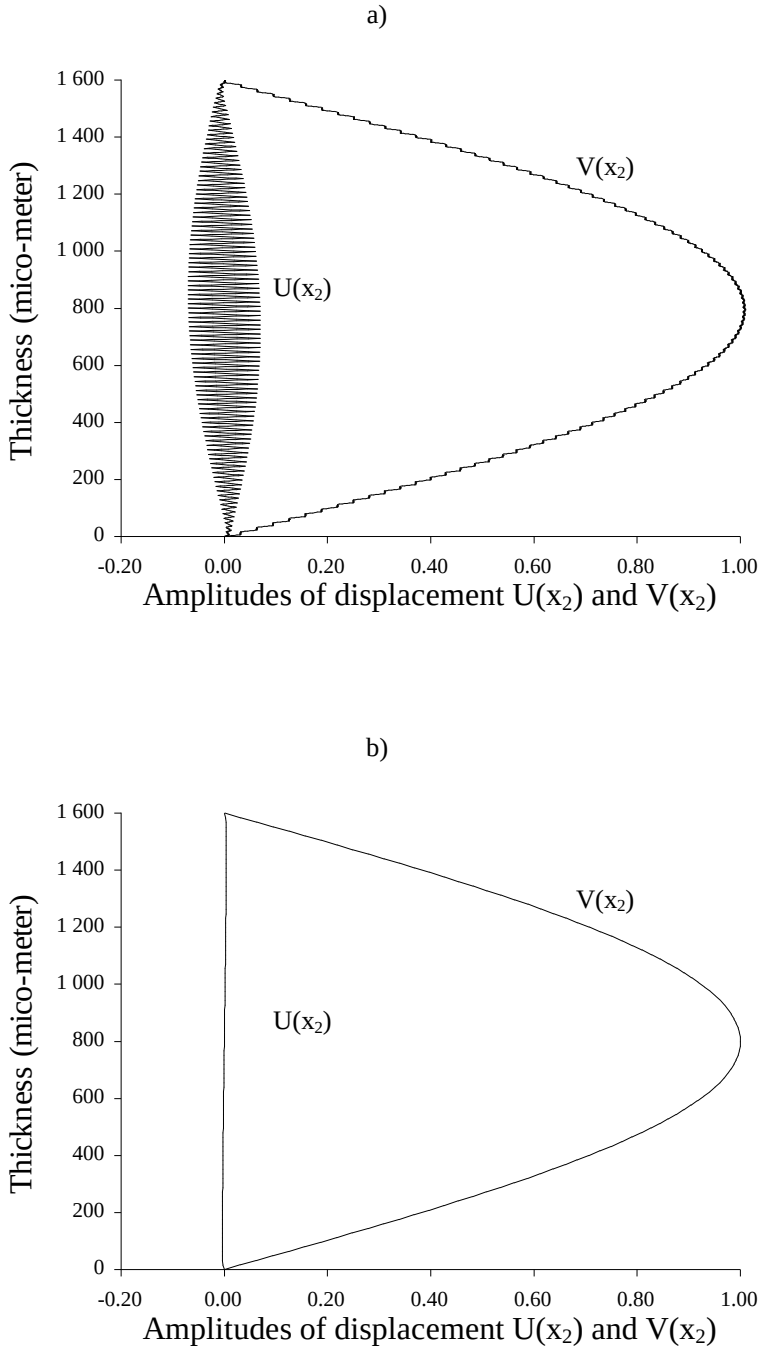

Figure 8 : Shape of amplitudes in the case of purely unidirectional composite, a) complete discretization, b) macroscopic model, thickness 1600 μm, boundary conditions : both clamped bottom and top faces.

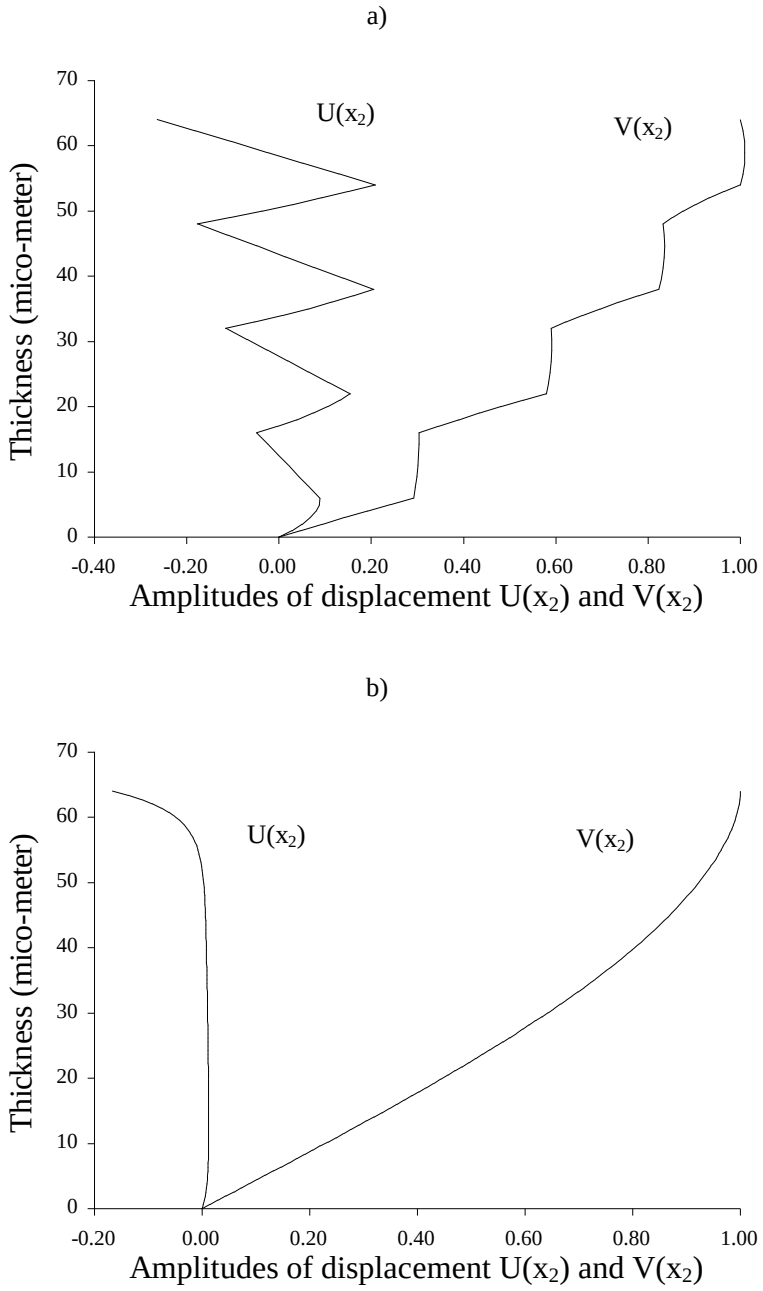

Figure 9 : Shape of amplitudes in the case of purely unidirectional composite, a) complete discretization, b) macroscopic model, thickness 64 μm, boundary conditions : clamped bottom face and free top face.

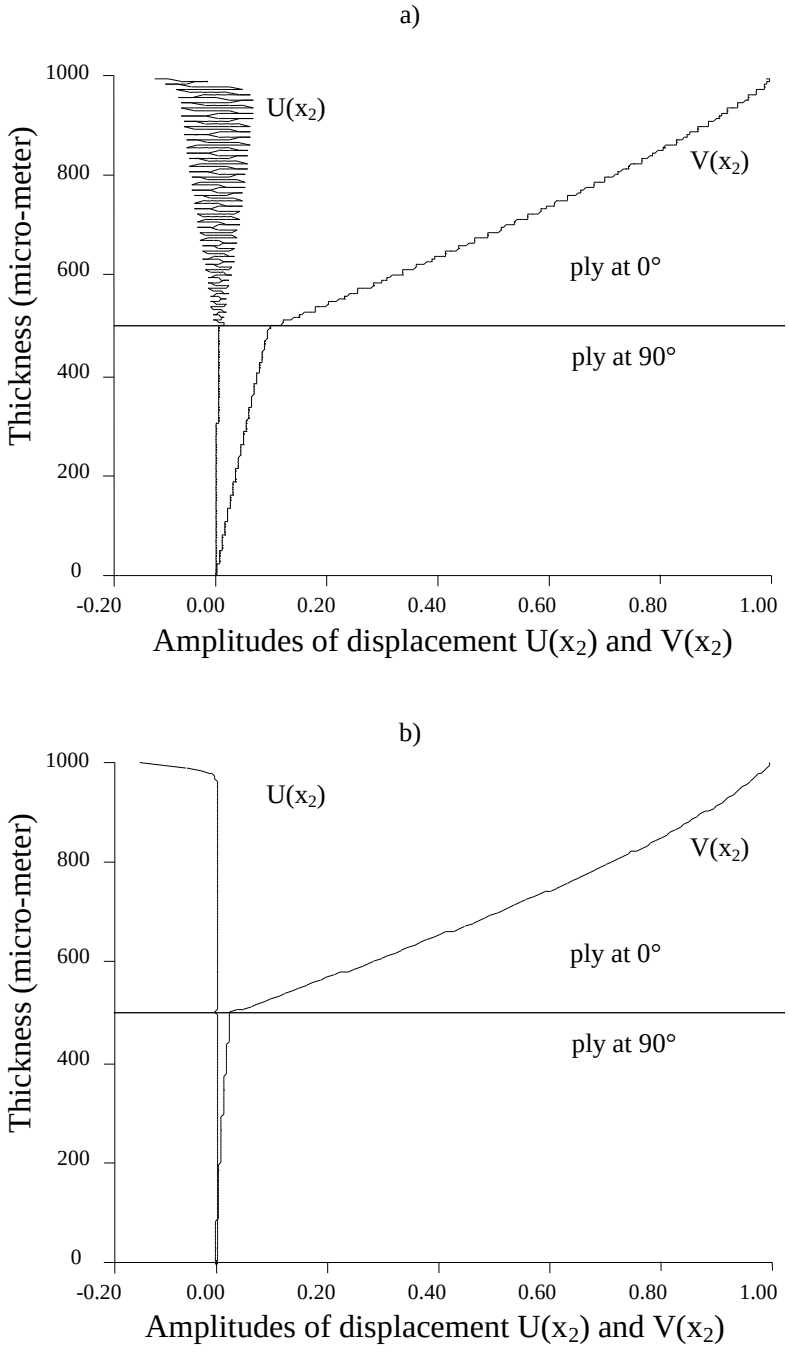

Figure 10 : Shape of amplitudes in the case of cross-ply laminate $[90_4,0_4]$, a) complete discretization, b) macroscopic model, thickness 1000 μm, boundary conditions : clamped bottom face and free top face.

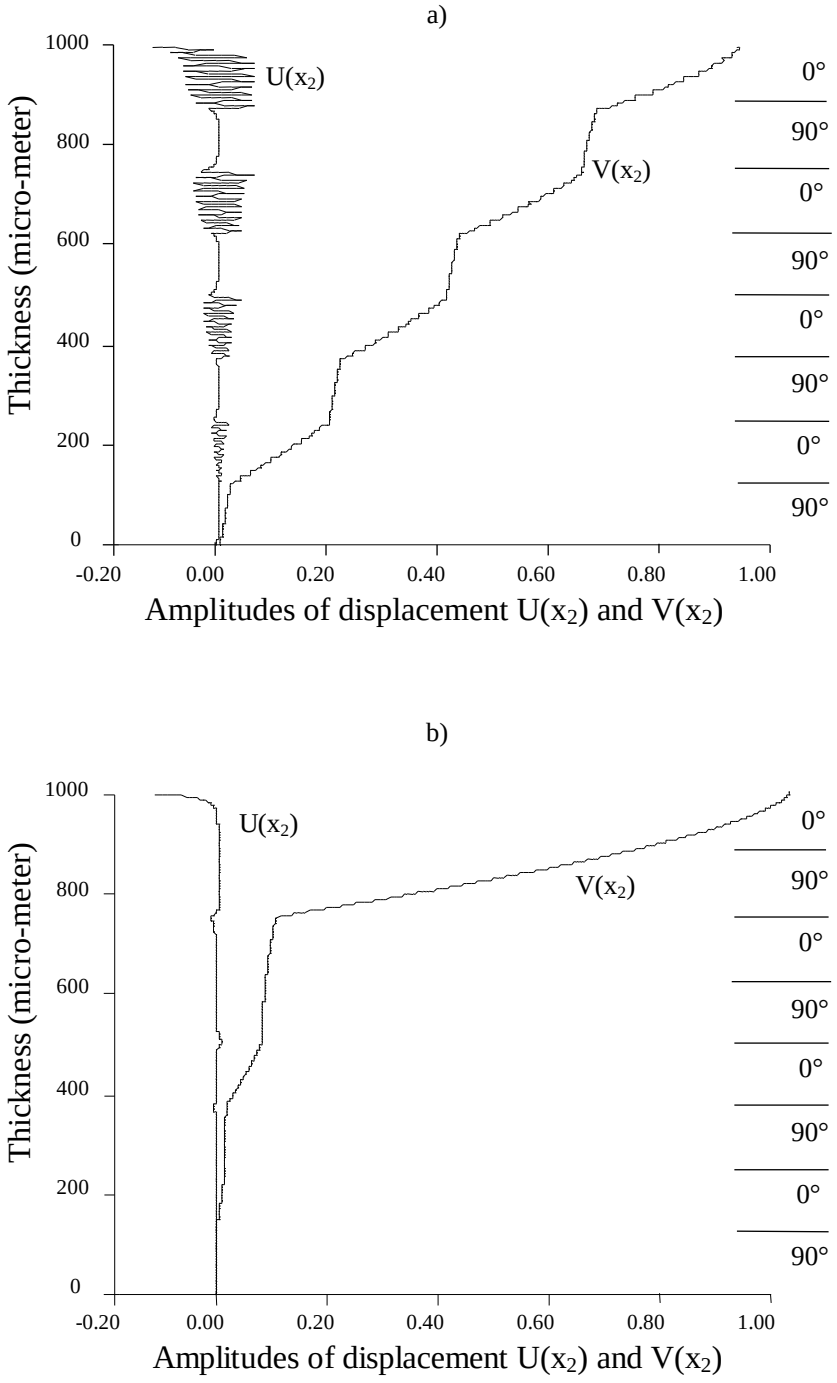

Figure 11 : Shape of amplitudes in the case of cross-ply laminate $[90,0]_4$, a) complete discretization, b) macroscopic model, thickness 1000 μm, boundary conditions : clamped bottom face and free top face.

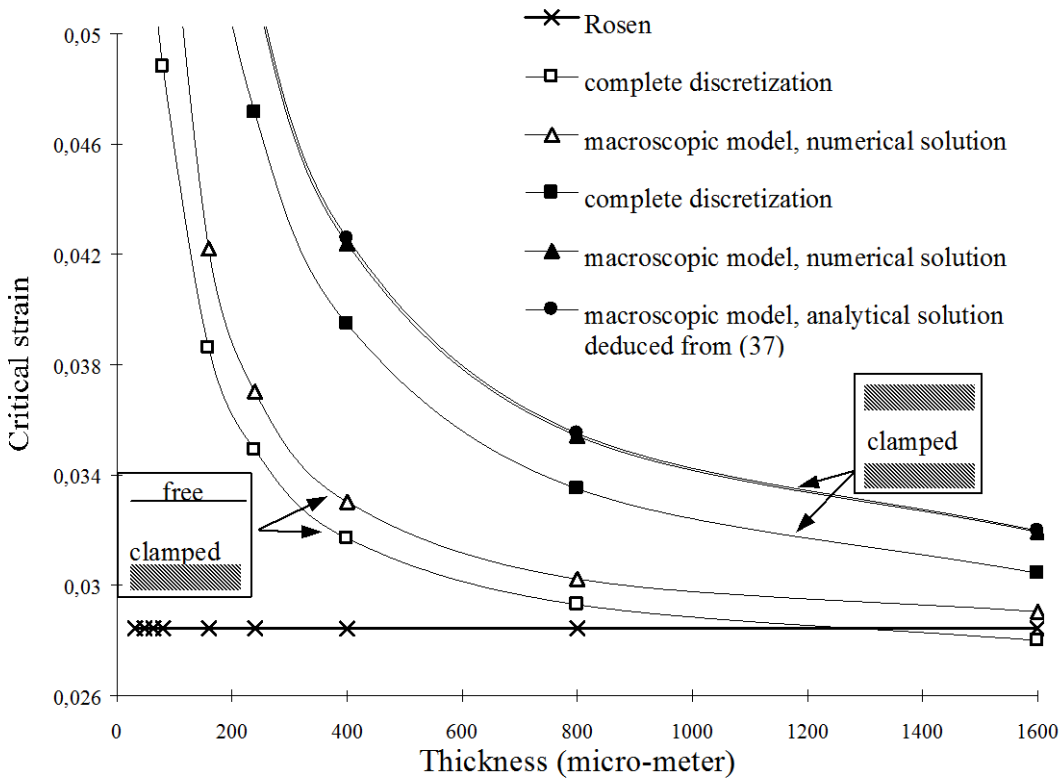

Figure 12 : Effect of the thickness and the boundary conditions on the critical strain.

This model has been validated in the case of 1000 μm thick laminates with two different stacking sequences : $[90_4,0_4]$ and $[90,0]_4$. The bottom face is clamped and the top face is free. For the $[90_4,0_4]$ laminate, the modes obtained by use of the homogenized model are similar to those calculated by complete discretization (Figure 10). On the other hand, the modes are slightly different in the case of the $[90,0]_4$ laminate (Figure 11). This difference is due to the representation of the 90° or 45° plies by classical 2-D equivalent homogeneous media, which supposes that the instability can appear only in 0° plies. The transverse plies behave then like elastic supports that are too stiff.

A set of calculations has been performed for different thickness and two types of boundary conditions (clamped bottom and free top faces, and both clamped bottom and top faces). In Figure 12, the critical strains calculated by the two approaches (homogenized model and heterogeneous model) are plotted versus laminate thickness. The critical strains are very close together for thick plies, while a slight difference is observed for thin plies (< 200 μm). The comparison between the wavelengths obtained by both models is excellent as proved in Figure 13 An particular example of numerical result is presented in the table 4.

To sum up, it is well established that our homogenized model is quite capable of representing the modes and the critical microbuckling strains and wavelengths which can appear in laminates. The structural effect is correctly represented, and the critical strains tend to the values given by Rosen's model for great ply thickness. These results show that the hypotheses made to build up the macroscopic model are sufficient.

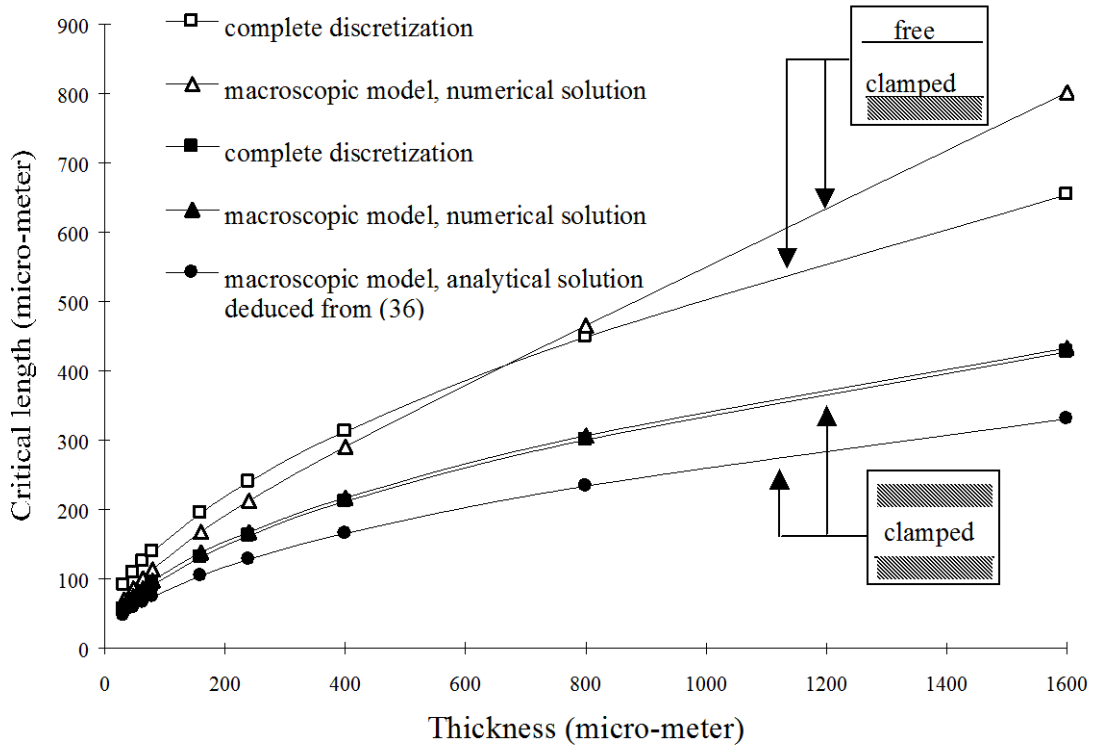

Figure 13 : Effect of the thickness and the boundary conditions on the critical wavelength.

Clamped-free	Heterogeneous model	Homogenized model (numerical solution)
Critical strain	2,82%	2,95%
Wavelength Wavenumber	654,50 μm k = 0,0096	661,4 μm 0.0095

Table 4 : Comparison of the heterogeneous and homogenized models.

5. CONCLUSION

In conclusion, our model is a classical non-linear elastic model, but which accounts for the fibre bending energy. An asymptotic study has permitted to lead to Rosen's model by removing all the dependences on the transverse variable. It was known that such a model should include both fibre bending stiffness and transverse stiffness (Gardin and Potier-Ferry [5], Swanson [7]). However with this approach, it is not possible to obtain the boundary layer which appear near the free faces. Consequently a two-dimensional model has been built by extending the results of the preceding

asymptotic study. The longitudinal displacement u is added to the asymptotic model in order to satisfy exactly the boundary conditions which are imposed on the ply faces.

The homogenized model is quite capable of representing the modes and predicts the critical microbuckling strains and wavelengths which can appear in purely unidirectional or laminated media. This is confirmed by numerical results on heterogeneous structures. The distribution of modal amplitudes is obtained in a satisfactory manner. The boundary layers, which concern only a few fibres, are well described by the model, in spite of its homogeneous feature. This is an important result, which shows that it is possible to model localized instability phenomena with a homogeneous model.

The effect of thickness and stacking sequence on instability (called structural effect) is correctly represented, and the critical strains tend to the values given by Rosen's model for great ply thickness. These results show that the hypotheses made to build up the macroscopic model are sufficient and coherent.

REFERENCES

1. Rosen B.W., Mechanics of composite strengthening, Fiber Composite Materials, American Society for Metals Seminar, Metal Parks, Ohio, pp. 37-75, (1964).
2. Schaffers W.J., Buckling in fiber-reinforced elastomers, Text. Res. J., p. 502-512, (1976).
3. Budiansky B., Micromechanics, Comp. and Struct., 16, pp. 3-12, (1983).
4. Grandidier J.C. and Potier-Ferry M., Microflambage des fibres dans un matériau composite à fibres longues, C. R. Acad. Sci. Paris, Série II, 310, pp. 1-6, (1990).
5. Gardin C. and Potier-Ferry M., Microflambage des fibres dans un matériau composite à fibres longues : analyse asymptotique 2-D, C. R. Acad. Sci. Paris, Série II, 315, pp. 1159-1164, (1992).
6. Guynn E.G., A parametric study of variables that affect fiber microbuckling initiation in composite laminates : Part I - Analyses, J. of Composite Materials, 26-11, pp. 1594-1616, (1992).
7. Swanson S.R., A micro-mechanics model for in-situ compression strength of fiber composite laminates, ASME J. Engng Mat. Tech., 114, pp. 8-12, (1992).
8. Budiansky B. and Fleck N.A., Compressive failure of fiber composites, J. Mech. Phys. Solids, 41, pp. 183-211, (1993).
9. Wisnom M.R., The effect of fiber waviness on the relationship between compressive and flexural strengths of unidirectional composites, J. of Composite Materials, 28, pp. 66-76, (1994).
10. Fleck N.A., Deng L. and Budiansky B., Prediction of kink width in fiber composites, J. Appl. Mech., 62, pp. 329-337, (1995).
11. Fleck N.A. and Shu J.Y., Microbuckle initiation in fibre composites : a finite element study, J. Mech. Phys. Solids, 43, pp. 1887-1918, (1995).
12. Kyriakides S., Arseculeratne R., Perry E.J. and Liechti K.M., On the compressive failure of fiber reinforced composites, Int. J. Solids Struct., 32(6/7), pp. 689-738, (1995).
13. Drapier S., Grandidier J.C., Gardin C. and Potier-Ferry M., Structure effect and microbuckling, Special JNC9, Comp. Sci. Tech., 56, pp. 861-867, (1996).
14. Drapier S., Grandidier J.C. and Potier-Ferry M., Theoretical study of structural effects on the compressive failure of laminate composites, C. R. Acad. Sci. Paris, Série IIb, 324, pp. 219-227, (1997).
15. Drapier S., Grandidier J.C. and Potier-Ferry M., Towards a numerical model of the compressive strength for long fibre composites, European Journal of Mechanics/A Solids, 18, pp. 785-790, (1999).
16. Koiter W.T., On the stability of elastic equilibrium, Thesis, Delft, Amsterdam. English translation

issued as Nasa TT F-10, 833, 1967, (1945).
17. Grandidier J.C., Ferron G. and Potier-Ferry M., Microbuckling and strength in long fiber composites : theory and experiments, Int. J. Solids Struct., 29, pp.1753-1761, (1992).
18. Grandidier J.C. and Potier-Ferry M., Microbuckling and homogenization for long fiber composites, Z.A.M.M., 71-4, pp. 371-374, (1991).
19. Sanchez-Palencia E., Non-homogeneous media and vibration theory, Lecture Notes in Physics, Springer Verlag, (1980).
20. Destuynder P., Une théorie asymptotique des plaques minces en élasticité linéaire, Ed. Masson, France, (1986).

ANNEXE : Detailed description of mode

Case of thick layer

From the numerical results, we have deduced a linear interpolation of the displacement field in the vicinity of x_2 equal to 1400 μm (Figure 14). They can be expressed as follows :

In the fibre

$$\begin{cases} u(x_1, x_2) = [- 0.925 \left(\frac{x_2 - 1419}{10} \right) + 0.039] \cos kx_1 \\ v(x_1, x_2) = 10.1 \sin kx_1 \end{cases}$$

In the matrix

$$\begin{cases} u(x_1, x_2) = [0.929 \left(\frac{x_2 - 1427}{6} \right) + 0.043] \cos kx_1 \\ v(x_1, x_2) = [0.097 \left(\frac{x_2 - 1427}{6} \right) + 10.147] \sin kx_1 \end{cases}$$

where the wavenumber k is equal to 0.0081.

The linearized strains are derived from this displacement field by classical formulas :

	In the fibre	In the matrix
ε_{11}	$[0.925 \left(\frac{x_2 - 1419}{10} \right) - 0.039] k \sin kx_1$ max. value : 0.00406	$[- 0.929 \left(\frac{x_2 - 1427}{6} \right) - 0.043] k \sin kx_1$ max. value : 0.00411
ε_{22}	$\leq 10^{-6}$	$\frac{0.097}{6} \sin kx_1$ max. value : 0.01617
ε_{12}	$\frac{1}{2} \left(- \frac{0.925}{10} + k\, 10.1 \right) \cos kx_1$ max. value : 0.00535	$\frac{1}{2} [\frac{0.929}{6} + k [0.097 \left(\frac{x_2 - 1427}{6} \right) + 10.147]] \cos kx_1$ max. value : 0.11871

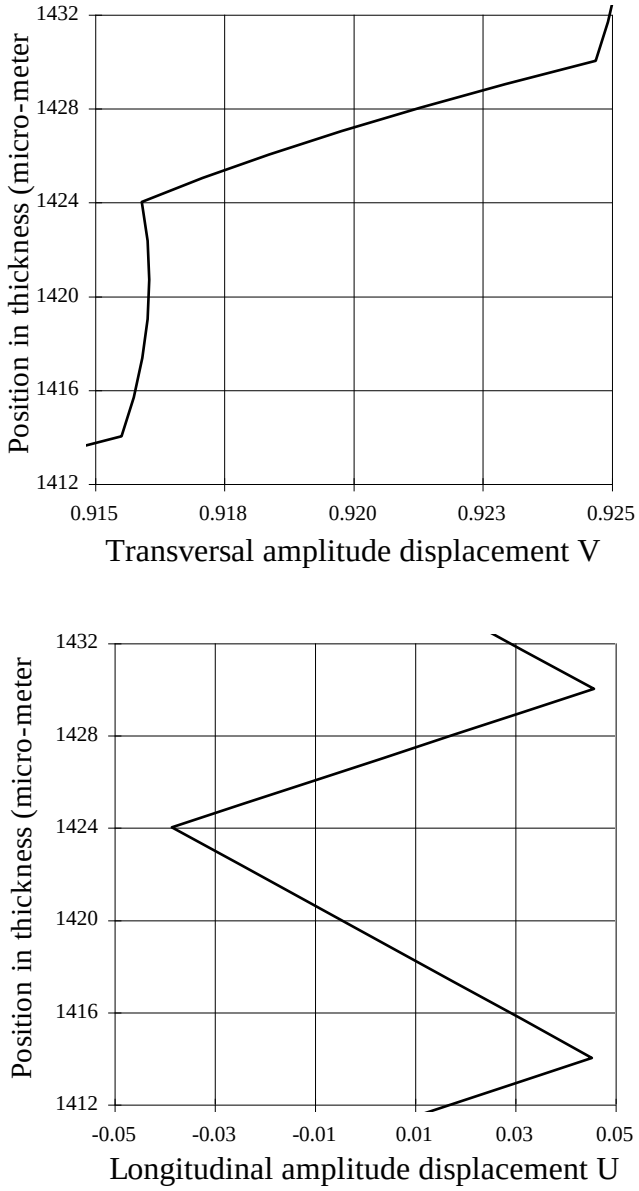

Figure 14 : Zoom of modal amplitudes, complete discretization, compressive load, thickness 1600 μm, boundary conditions : clamped bottom face and free top face.

Case of thin layer

In the case of a 160 μm layer, we have also done a linear interpolation, even if the shape seems slightly different (see Figure 15). The following approximations are considered in the vicinity of x_2 equal to 140 μm, for the sake of similitude with the previous case:

In the fibre
$$\begin{cases} u(x_1, x_2) = [- 2.659 \left(\frac{x_2 - 139}{10} \right) + 0.027] \cos kx_1 \\ v(x_1, x_2) = 8.8 \sin kx_1 \end{cases}$$

In the matrix

$$\begin{cases} u(x_1, x_2) = [\, 2.299 \left(\frac{x_2 - 147}{6}\right) - 0.125 \,] \cos kx_1 \\ v(x_1, x_2) = [\, 0.484 \left(\frac{x_2 - 147}{6}\right) + 8.906 \,] \sin kx_1 \end{cases}$$

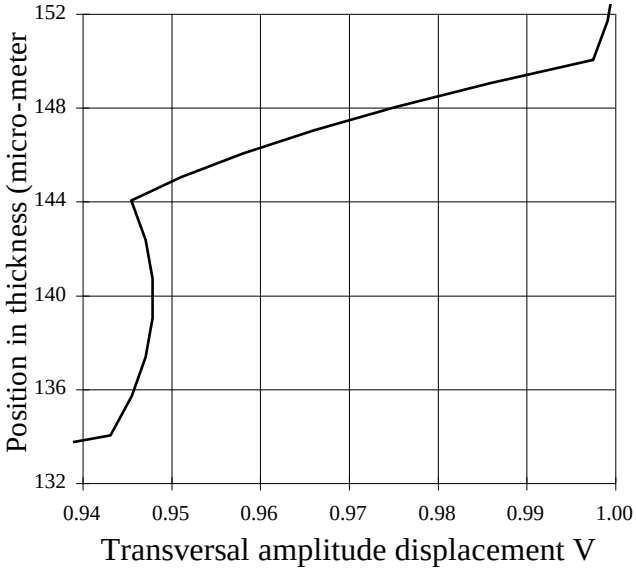

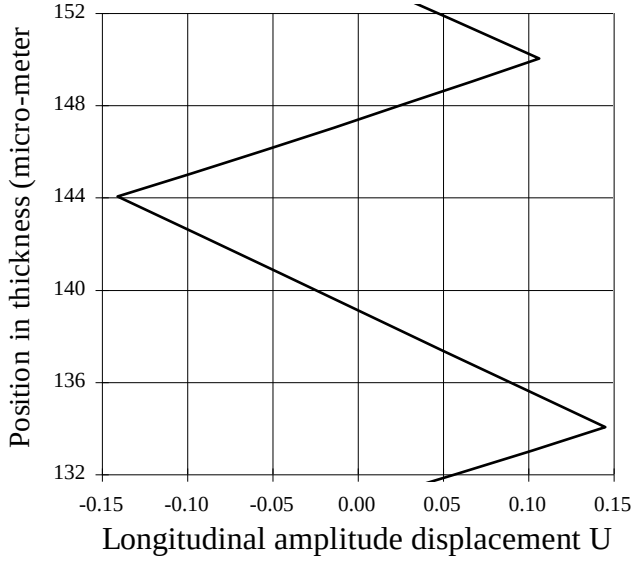

Figure 15 : Zoom of modal amplitudes, complete discretization, compressive load, thickness 160 μm, boundary conditions : clamped bottom face and free top face.

Let us recall by the way that an instability mode is an eigenvector that can be multiplied by an

arbitrary constant. In the preceding relations, the wavenumber k is equal to 0.0411, the critical microbuckling strain is equal to 4.43%, and the wavelength is equal to 153 μm. The strains are calculated as previously, which gives :

	In the fibre	In the matrix
ε_{11}	$[\ 2.659\ (\ \frac{x_2 - 139}{10}\ )\ -\ 0.027\ ]\ k\ \sin kx_1$ max. value : 0.05353	$[\ -\ 2.299\ (\ \frac{x_2 - 147}{6}\ )\ +\ 0.125\ ]\ \ k\ \sin\ kx_1$ max. value : 0.05238
ε_{22}	$\leq 10^{-6}$	$\frac{0.484}{6}\ \sin\ kx_1$ max. value : 0.0807
ε_{12}	$\frac{1}{2}(\ -\ \frac{2.659}{10}\ +\ k\ 8.8\ )\ \ \cos\ kx_1$ max. value : 0.04789	$\frac{1}{2}\ [\ \frac{2.299}{6}\ +\ k\ [0.484\ (\ \frac{x_2 - 147}{6}\ )\ +\ 8.906]\ ]\ \cos kx_1$ max. value : 0.37957